Oil Dispersion with a Turbine Mixer

R. R. ROUNSLEY

Mead Corp.
Chillicothe, OH 45601

A laboratory study was conducted to determine the factors influencing the dispersion of oil with a turbine mixer. Drop-size distributions as a function of time were related to the impeller diameter, power expended in relation to the liquid volume, and the final emulsion temperature.

It was surprising that higher temperatures produced smaller mean drop diameters but at the expense of a wider distribution. An optimal batch size for the emulsion was found to exist in processing. Below this size, tank surface and internal turbulence waste much of the energy; above this size, the energy per unit volume became a critical factor.

Other trials were made to determine the effect of the turbulence of the tank surface, tank geometry, number of impeller blades, and turbine configuration. These all significantly affect drop size and should be considered in the design and selection of dispersing equipment.

SCOPE

The emulsification of oil with a turbine mixer in a baffled cylindrical tank was correlated for the Sauter mean diameter as a function of time. Several time relationships are considered which describe the resulting mean drop diameter. The ultimate diameter that can be reached at infinite dispersion time is correlated to the operating conditions.

A size distribution computer program is described and applied to the measured emulsification data. Mean diameters in the range of 1 to 30 μm were evaluated. An analysis is made of the emulsion size distributions for the emulsions and the conditions which formed them.

Several different types and sizes of impellers were employed and these are evaluated on their ability to produce a desired size distribution rapidly. Different emulsion levels in the tank are related to the effective use of agitator power.

CONCLUSIONS AND SIGNIFICANCE

Emulsification conditions and the time to produce a given Sauter mean diameter can be described by several relations. The simplest of these describes the mean diameter as a function of the power expended and time and is in the form:

$$d_{32} = \frac{0.02203|V - 18.93|^{0.45}}{d_I^{4.41} N^{3.50} T^{0.573} t^{0.400}}$$

The confidence limits on d_I and N include the power number exponents $\{d_I^5 N^3\}$ exponent as observed by Thornton and Buoyatiotis (1963). The equation is significant above the 99% level having an F test of 30.8. This equation applies in our system to a six-bladed flat turbine in a baffled tank.

It was observed that higher temperatures (lower viscosity and surface tensions) produced smaller drop diameters as indicated, but this was at the expense of wider distribution which is not shown by the equation.

A more accurate measure of change in particle size with time may be obtained by plotting the mean diameter against the reciprocal of time. This results in a straight line for times greater than two hours for our system. The intercept ($t = \infty$) is the smallest mean diameter that can be produced under these emulsifying conditions. When the difference between actual and ultimate diameter is plotted on semilog paper, a straight line results for all observations. This provides an accurate way to predict mean drop diameter with time when the ultimate diameter for particular operation is known. A correlation of the ultimate diameter and emulsification conditions has been determined.

An optimum batch size for emulsion production was determined to exist in the tank. This optimum occurred when the level in the tank was roughly equal to the tank diameter. Below this level, turbulence of the tank surface wasted much of the energy; above this level, the energy per unit volume decreased markedly.

Other trials were made to determine the effect of turbulence of the tank surface, the number of impeller blades, and turbine configuration. These all significantly affect drop size and should be considered in the design of dispersion equipment.

BACKGROUND

In the production of large emulsion sizes in the range of 1,000 μm and larger, the effect of coalescence is pronounced as described by Brodkey (1967). In contrast, Shinnar (1961) was able to control coalescence by surface active agents and showed that the Sauter mean diameter of an emulsion produced was proportional to the impeller speed to $-3/4$ power. On the other hand, Sprow (1967) measured emulsion diameters near a turbine impeller in dilute iso-octane and salt water emulsion. These samples showed little coalescence and gave an impeller speed exponent of $-6/5$ power.

Mlynek and Resnick (1972) used water and a mixture of iso-octane and carbon tetrachloride in which there was no dependence of drop size on location in the vessel. They concluded that the mean emulsion diameter was correlated with the Weber number $(N^2 d_I^3 \rho/\sigma)$ to the -0.6 power.

Droplet-size distributions in a baffled vessel were determined by Thornton and Bouyatiotis (1963). Drop-size distributions were given at zero holdup as a correlation containing power per unit

volume cubed in a dimensionless group to the −0.32 power. The net result is an exponent on the power/volume term of −0.96.

We have been concerned with the production of emulsions with mean diameters of 1 to 10 μm. In this size range, the emulsion behaves more nearly like solid particles with little coalescence. These emulsions are produced at high volume fractions of the dispersed phase at 38.9%. Although some of these authors cited investigated emulsions with low coalescence, few studies have been done at high-volume fractions.

In addition, there was also a particular interest in the drop-size distribution produced in these studies. Both Lapple (1963) and Keey and Glen (1969) reported diameter-frequency plots which show a logarithmic-normal distribution for drop size. The geometric deviation, which is the ratio of the particle sizes within a simple standard deviation, was observed to fall between 2 and 3. A narrow distribution will have a large geometric deviation.

Chang, Sheu, Tatterson and Dickey (1980) and Van 't Riet (1975) have shown that the breakup of an emulsion occurs near the impeller. All agitators shed vortices from the tips of the impeller blades under the turbulent flow conditions. In high-speed stereo films of the phenomena by Tatterson, the large drops of oil can be seen to stretch and break up in the vortex. This was the only place the breakup occurred. Except under extreme conditions, the flow regime at the tip of the impeller blades controls the vortex formation and, therefore, the rate of emulsification.

The impeller in any mixing application has two functions: pumping and turbulence. Gross turbulence is largely the result of the pumped fluids interacting with the baffles and walls. Localized turbulence is the result of the vortices shed by the impeller. Both functions require energy from the impeller. Fondy (1963) has shown the ultimate diameter of emulsion produced is controlled solely by tip speed of the impeller with a given emulsion at constant temperature. Most of the energy consumption, on the other hand, seems to go into moving (pumping) the fluid and in gross turbulence. However, for breakup of a drop in an emulsion, energy must be put into the drop to overcome surface and viscous forces. This is a difficult task and therefore emulsification is very energy-inefficient. Fondy recommends that the impeller diameter be reduced to minimize power consumption since the pumping action increases dramatically with the impeller diameter. Van't Riet (1975) has estimated that only 10% of the fluid pumped passes through the high shear region. Finally Rushton (1977) states that dimensionless groups generally used to describe mixing and fluid flow do not fully account for the interactions affecting emulsification.

PROCEDURES

The emulsification work was performed on a specially designed test stand with a 0.75-hp (0.56-kW) variable speed mixer. This allowed the application of relatively large power input into the 35-L baffled glass tank. The mixer motor and impeller could be moved up and down on the stand with a counterbalance arrangement so that the impeller could be precisely located above the bottom of the tank. The tank itself was located in the center of a turntable mounted on roller bearings. The torque transmitted to the tank could be measured with a spring scale connected to a 231.8-mm torque arm from the turntable. The tank was strapped to a support on the turntable.

Four impellers were used: three flat blade turbines and a marine impeller. The flat blade turbines were 114.3 and 152.4 mm in diameter and 25 to 35 mm wide. The 152.4 mm (35 mm wide) turbine had six blades while one 114.3-mm turbine had six blades 25 mm wide and the other had 12 blades. The marine impeller was 114.3 mm in diameter.

The tank diameter was 285 mm and had four 25-mm baffles attached and extending to about 12 mm from the tank bottom. The ratio of baffle width to tank diameter therefore was about 11.5. Total tank height was 610 mm although the largest emulsion batch used was 26.5 L extending only 410 mm up the wall.

The water-base polymer solution of about 0.220 Pa·s viscosity was poured into the tank, then the impeller was adjusted to about 90 mm off the bottom to prevent air entrainment during the addition of oil. The oil to be emulsified consisted of a mixture of about 60% aromatic hydrocarbon diluted with kerosene having a specific gravity of about 1.0. The oil viscosity was 0.008 to 0.010 Pa·s, and it was completely immiscible in the water solution. It was stored in a plastic tank from which it could be metered slowly through plastic tubing into the mixing tank to give 38.8% oil by weight (and volume) over a period of 10 to 20 minutes. The oil was added at such a location that it was immediately drawn into the turbine for initial dispersion. Once all of the oil was added, the turbine height was adjusted to one-third the distance from the tank bottom to the emulsion surface. Batch samples were taken from the rapid moving portion of the tank. It was found the mean drop sizes of the samples taken before 60 minutes were not stable. Consequently, the first recorded samples were taken 90 minutes after the start of oil addition. No coalescence was observed in the samples taken after 90 minutes. The samples were diluted and analyzed immediately on the Coulter counter. A data summary is given in Table 1. The data are for the turbine impellers except where marked as being for the marine impeller.

The temperature of the emulsion was measured as each sample was removed. Since most of the mixing energy ended up in emulsion, the temperature tended to rise. At higher impeller speeds, this became a problem. Therefore, a number of runs were made with the temperature of the tank controlled by a water jacket around the tank to account accurately for these variations.

SIZE DISTRIBUTIONS

A computer program was written to take each of the volumetric particle-size distributions from the Coulter counter and convert it to surface-area-weighted distribution from which the Sauter mean diameter was obtained. The cumulative distribution from the Coulter counter was converted to a probability log-diameter function to describe the distribution. An example of the output from this program for Batch 9 at 300 minutes mixing time is given in Table 2. The converted diameter and its log for each of the fractions is shown (by surface area). These fractions are converted to probabilities measured as the number of standard deviations above or below the mean where they lie. Thus, 68.3% of the particles lie within one standard deviation of the mean; 95.5% lie within two sigma. When these data are correlated statistically, the intercept of the regression represents the log of median diameter. This diameter along with the Sauter mean are given. For a perfect fit of the data, tese two diameters will be the same.

When the data are actually plotted on probability paper, Figure 1, it is evident that the data above the median and the data below the median form two distinct groups. This has been observed by other experimenters. Each half can be correlated in a similar manner giving two best lines. The slopes of both of these are given in addition to their intercept (median). For a perfect fit, again, these three lines would be the same. To compare them, a t-test is given for each of the lines. A t-value greater than 2.5 is significant at the

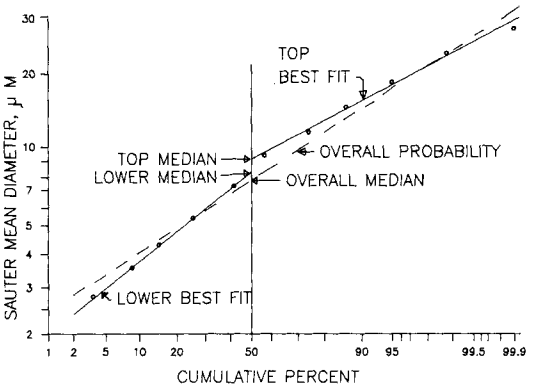

Figure 1. Typical probability curve, Run 9, 300 minutes.

TABLE 1. TURBINE MIXING TRIALS, DATA SUMMARY

Turbine Dia., mm	Batch Size L	Speed s^{-1} (m/s)	Power W	Temp. °C	Time min	d_{32} μm	Slope Dstrb	Slope Bottom	Slope Top	Slope d_{32}-T m·s	Time Const. s
Run 9											
152.4	18.9	9.17	197	37.0	90.0	18.79	0.3893	0.6251	0.2266		
			201	42.0	150.0	13.66	0.4530	0.5615	0.3128		
			204	46.0	210.0	10.88	0.4448	0.6014	0.3063		
			201	49.0	300.0	8.13	0.4873	0.6132	0.3954		
	Tip Speed	(4.39)			Ult.	3.05				0.0956	3,546
Run 10	Early Samples Unstable										
152.4	11.4	7.5	67	36.0	300.0	29.14	0.3819	0.6010	0.2463		
			67	36.0	330.0	26.69	0.4266	0.6152	0.2694		
		(3.59)			Ult.	24.73				0.0600	8,100
Run 11											
152.4	11.4	10.83	162	40.0	90.0	9.99	0.4363	0.6045	0.3536		
			162	43.0	150.0	7.59	0.4743	0.5425	0.4298		
			162	46.0	210.0	5.81	0.4863	0.5588	0.4763		
			162	46.0	300.0	4.25	0.4785	0.5144	0.4968		
		(5.19)			Ult.	0.88				0.0610	4,560
Run 13											
152.4	26.5	9.17	234	36.0	90.0	17.13	0.3601	0.5396	0.2587		
			230	41.0	150.0	15.77	0.4110	0.5458	0.2980		
			230	46.0	210.0	13.82	0.4554	0.5891	0.3519		
			233	50.0	300.0	9.16	0.4501	0.2379	0.5361		
		(4.39)			Ult.	4.75				0.0995	3,612
Run 14	Mixer Speed Surging										
152.4	18.9	9.17	208	37.0	90.0	12.43	0.5023	0.5546	0.3927		
			204	41.0	150.0	10.26	0.5513	0.7053	0.4466		
			204	44.0	210.0	9.03	0.5746	0.6389	0.5002		
			204	46.0	300.0	7.24	0.5464	0.6893	0.4804		
		(4.39)			Ult.	3.91				0.0602	4,596
Run 15											
152.4	11.4	9.17	130	35.0	90.0	16.85	0.4267	0.6468	0.2663		
			130	40.0	150.0	14.75	0.4998	0.6619	0.3338		
			122	42.0	210.0	10.83	0.4406	0.6542	0.3703		
			122	43.0	300.0	8.98	0.4649	0.5894	0.3571		
		(4.39)			Ult.	3.86				0.0934	3,636
Run 16											
152.4	18.9	9.17	204	37.0	90.0	10.36	0.4717	0.6774	0.3569		
			204	42.0	150.0	8.27	0.5205	0.6610	0.4269		
			212	46.0	210.0	7.59	0.4635	0.5392	0.4065		
			212	48.0	300.0	5.46	0.5201	0.5918	0.4822		
		(4.39)			Ult.	3.06				0.0494	5,364
Run 17	First Samples Were Lost										
152.4	26.5	7.5	128	38.0	210.0	24.47	0.3378	0.4509	0.2652		
			125	40.0	300.0	23.34	0.3294	0.4746	0.2431		
		(3.59)			Ult.	20.52				0.0502	9,012
Run 18	Lost Baffle At 225 Min.										
152.4	18.9	10.83	298	40.0	90.0	5.70	0.5431	0.5904	0.5523		
			298	50 0	150.0	3.92	0.5620	0.6084	0.5216		
			298	56.0	210.0	2.95	0.5354	0.6375	0.4891		
			298	56.0	300.0	2.43	0.5338	0.6168	0.4641		
		(5.19)			Ult.	1.01				0.0254	9,966
Run 19	Rerun No. 12										
152.4	18.9	7.50	110	34.0	90.0	21.89	0.4649	0.6694	0.3375		
			110	36.0	150.0	18.43	0.4891	0.6794	0.3694		
			110	36.0	210.0	16.10	0.5288	0.7566	0.4042		
			110	36.0	300.0	14.27	0.4918	0.4634	0.4423		
		(3.59)			Ult.	10.26				0.0733	4,080
Run 20	Alternate Turbine										
152.4	18.9	9.17	216	40.0	90.0	9.28	0.5489	0.6190	0.4791		
			216	49.0	210.0	5.41	0.5689	0.5881	0.5769		
			216	51.0	300.0	3.72	0.5976	0.8185	0.5054		
										0.0695	
Run 21	Reduced Speed to Hold Temp. Constant										
152.4	26.5	10.00	324	30.0	90.0	10.44	0.4878	0.6019	0.3981		
			324	39.0	150.0	8.87	0.5381	0.6451	0.4748		
			324	48.0	210.0	7.30	0.5524	0.6783	0.4791		
			324	58.0	300.0	5.77	0.5502	0.5881	0.5373		
		(4.79)			Ult.	2.76				0.0556	4,896
Run 25	With Floating Cover										
152.4	18.9	9.17	197	38.0	90.0	5.26	0.4551	0.2475	0.6635		
			208	44.0	150.0	6.54	0.5101	0.5402	0.4731		
			208	48.0	210.0	5.39	0.5584	0.5761	0.5716		
			208	49.0	300.0	4.31	0.5199	0.5804	0.5150		
										0.0402	

TABLE I *Continued*

Turbine Dia., mm	Batch Size L	Speed s^{-1} (m/s)	Power W	Temp. °C	Time min	d_{32} μm	Slope Dstrb	Slope Bottom	Slope Top	Slope d_{32}-T m·s	Time Const. s
Run 33	Alternate Turbine										
152.4	18.9	9.17	193	34.0	90.0	15.81	0.4516	0.6461	0.3391		
			202	40.0	150.0	10.12	0.4656	0.5948	0.3533		
			193	44.0	210.0	7.27	0.4880	0.6367	0.3782		
			202	47.0	300.0	5.29	0.5043	0.7119	0.3758		
										0.0870	
Run 22											
114.3	18.9	12.22	148	36.0	90.0	13.57	0.4972	0.6813	0.3880		
			154	40.0	150.0	11.01	0.5512	0.6247	0.4841		
			154	44.0	210.0	8.88	0.5443	0.6966	0.4741		
			159	46.0	300.0	7.76	0.5510	0.5484	0.5352		
		(4.38)			Ult.	4.05				0.0630	4,434
Run 23	Marine Propeller										
114.3	18.9	12.22	143	34.0	90.0	15.57	0.4766	0.7374	0.3098		
			143	39.0	150.0	12.53	0.4966	0.5438	0.3902		
			143	42.0	210.0	9.83	0.5512	0.6948	0.4500		
			143	45.0	300.0	8.04	0.5480	0.6668	0.4734		
										0.0822	
Run 24	Marine Propeller										
114.3	18.9	12.22	148	36.0	90.0	18.17	0.4556	0.6042	0.3897		
			154	40.0	150.0	15.94	0.4709	0.4853	0.4029		
			154	44.0	210.0	13.36	0.4770	0.5413	0.4101		
			148	46.0	300.0	10.53	0.6022	0.7306	0.5204		
		(4.38)			Ult.	6.29				0.0852	3,840
Run 27											
114.3	26.5	12.22	148	33.0	90.0	26.56	0.3157	0.4589	0.2240		
			158	36.0	150.0	23.99	0.3190	0.4834	0.2436		
			158	38.0	210.0	21.12	0.3345	0.4379	0.2171		
			158	40.0	300.0	17.79	0.3266	0.5653	0.2291		
		(4.38)			Ult.	12.41				0.1044	3,450
Run 28											
114.3	18.9	14.45	263	43.0	90.0	5.58	0.4587	0.5423	0.3748		
			263	46.0	150.0	4.20	0.4386	0.5642	0.3941		
			263	52.0	210.0	3.43	0.4922	0.5258	0.5110		
			269	54.0	300.0	3.52	0.3655	0.2498	0.4459		
		(5.19)			Ult.	1.65				0.0252	9,432
Run 31											
114.3	18.9	14.45	216	38.0	90.0	16.71	0.3627	0.5419	0.2574		
			228	42.0	150.0	10.20	0.4214	0.6235	0.3541		
			228	47.0	210.0	7.36	0.4504	0.5305	0.4225		
			228	51.0	300.0	5.03	0.4499	0.6268	0.3518		
		(5.19)			Ult.	0.15				0.0912	3,624
Run 32	High Torque Fluctuations										
114.3	11.4	12.21	91	30.0	90.0	19.27	0.4393	0.5973	0.3167		
			87	33.0	150.0	13.99	0.4440	0.6435	0.2828		
			87	33.0	210.0	11.85	0.4258	0.5810	0.3009		
			87	35.0	300.0	9.51	0.4261	0.6004	0.3472		
		(4.39)			Ult.	6.17				0.0684	426
Run 35	Repeat 31 With Cooling Jacket										
114.3	18.9	14.45	246	30.0	90.0	12.72	0.3848	0.6164	0.2688		
			251	33.0	150.0	9.85	0.4272	0.5135	0.3121		
			246	36.0	210.0	7.86	0.4066	0.6188	0.3046		
			251	35.0	300.0	6.33	0.4370	0.6128	0.3486		
		(5.19)			Ult.	3.54				0.0546	4,944
Run 36	Repeat 22 With Cooling Jacket										
114.3	18.9	12.21	158	24.0	90.0	17.23	0.3116	0.5094	0.2004		
			158	25.0	150.0	14.75	0.3769	0.5780	0.2434		
			163	26.0	210.0	13.49	0.5385	0.2319			
			163	26.0	300.0	12.38	0.3596	0.4650	0.2337		
		(4.39)			Ult.	10.39				0.0384	6,432
Run 38	With Floating Cover										
114.3	18.9	14.45	251	31.0	90.0	8.20	0.4423	0.4506	0.3300		
			270	33.0	150.0	5.86	0.4653	0.5284	0.3459		
			251	34.0	210.0	4.74	0.4658	0.6508	0.3643		
			257	34.0	300.0	4.11	0.4814	0.5802	0.3985		
										0.0330	
Run 40	Repeat 35 With Cooling										
114.3	18.9	12.21	158	35.0	90.0	13.11	0.4769	0.6178	0.3301		
			158	40.0	150.0	11.26	0.4420	0.5220	0.3407		
			163	43.0	210.0	9.60	0.4575	0.6204	0.3364		
			163	45.0	300.0	8.27	0.4464	0.4406	0.3972		
										. . .	
Run 41	12 Blade Impeller										
114.3	18.9	12.21	218	35.0	90.0	9.15	0 4932	0.6884	0.3608		

TABLE I *Continued*

Turbine Dia., mm	Batch Size L	Speed s^{-1} (m/s)	Power W	Temp. °C	Time min	d_{32} μm	Slope Dstrb	Slope Bottom	Slope Top	Slope d_{32}-T m·s	Time Const. s
			218	42.0	150.0	7.34	0.4750	0.6054	0.3763		
			218	45.0	210.0	6.32	0.5130	0.5423	0.4063		
			218	48.0	300.0	5.12	0.5278	0.6736	0.4325		
										0.0348	
Run 42	12 Blade, High Temp.										
114.3	18.9	14.45	351	44.0	90.0	4.80	0.5293	0.7097	0.4162		
			351	53.0	150.0	3.63	0.5392	0.6450	0.4743		
			351	58.0	210.0	3.00	0.5421	0.6169	0.5128		
			351	61.0	300.0	2.56	0.6271	0.6614	0.5589		
										0.0180	
Run 43	12 Blade, Reduced Speed										
114.3	18.9	10.0	125	28.0	90.0	29.19	0.3460	0.4518	0.2227		
			125	33.0	150.0	21.80	0.4319	0.6272	0.2633		
			122	36.0	210.0	18.91	0.4183	0.6104	0.2702		
			125	39.0	300.0	15.58	0.4449	0.6444	0.3183		
										0.1326	
Run 44	12 Blade, With Cooling										
114.3	18.9	14.45	357	38.0	90.0	4.87	0.5000	0.6878	0.3904		
			357	39.0	150.0	3.94	0.4694	0.5498	0.3777		
			357	45.0	210.0	3.30	0.4634	0.5820	0.3846		
			357	50.0	300.0	2.69	0.4434	0.5963	0.3948		
										0.0270	
Run 45	12 Blade, With Cooling										
114.3	18.9	12.22	257	38.0	90.0	8.93	0.4977	0.6434	0.3949		
			218	43.0	150.0	7.22	0.4834	0.5958	0.4201		
			222	46.0	210.0	6.23	0.5029	0.6089	0.4567		
			218	49.0	300.0	4.82	0.5457	0.7037	0.4687		
										0.0516	
Run 46	Alternate Blades Trimmed										
114.3	18.9	12.22	158	31.0	90.0	10.90	0.6016	0.6111	0.7071		
			158	36.0	150.0	8.34	0.4741	0.5082	0.3759		
			158	39.0	210.0	6.31	0.5040	0.5528	0.3681		
			163	41.0	300.0	5.30	0.5003	0.6335	0.3867		
										0.0630	
Run 48	Alternate Blades Trimmed										
114.3	18.9	14.45	269	40.0	90.0	5.35	0.4541	0.6615	0.3289		
			275	45.0	150.0	3.82	0.4743	0.5891	0.4056		
			275	49.0	210.0	3.07	0.4777	0.5984	0.4277		
			275	52.0	300.0	2.46	0.5118	0.5727	0.5101		
										0.0330	
Run 49	Alternate Blades Trimmed										
114.3	18.9	12.22	158	32.0	90.0	15.67	0.4385	0.6119	0.2977		
			158	36.0	150.0	10.69	0.4453	0.6667	0.3706		
			158	39.0	210.0	8.39	0.4673	0.5195	0.3630		
			158	42.0	300.0	6.91	0.4592	0.5741	0.3979		
										0.0828	

98% level. All data were correlated much better when treated in two segments, and the bottom of the curve invariably produced a larger t-test (Table 2) as shown in the example. Inspecting the summary of the data in Table 1 shows that the overall slope of the distribution generally became larger (wider distribution) as agitation time increased. On further inspection, the distribution or slope of the top half of the emulsion increased considerably as emulsification continued. Since the median diameter is different for each of these, what appears to be happening is that the more narrow distribution of the larger particles is being preferentially broken down into the smaller ones. The smaller particles already present are changed very little. This process will continue until an ultimate particle diameter is reached.

TABLE 2. SAMPLE OF EMULSION ANALYSIS

Batch 9, 300 min, Batch Size—18.91, Speed—9.17 rps, 150-mm diameter flat-blade turbine
Tip Speed = 4.39 m/s
0.269 measured hp input, power/volume—10.60 W/L
Emulsion Distribution Analysis

Mean Diameter	Log Dia.	Area-Weighted Fraction	Prob. Function
28.5096	3.3502	0.0011	3.0568
22.6513	3.1202	0.0115	3.2699
17.9778	2.8891	0.0509	1.6371
14.2548	2.6571	0.1313	1.1222
11.3144	2.4261	0.2807	0.5794
8.9800	2.1950	0.4536	0.1172
7.1274	1.9639	0.3914	−0.2740
5.6572	1.7329	0.2520	−0.6674
4.4900	1.5019	0.1506	−1.0352
3.5609	1.2700	0.0799	−1.4075
2.8264	1.0390	0.0368	−1.7895

Sauter Mean Diameter: 8.13. Median Diameter: 7.65.
68% of Particles Fall between 4.70 and 12.46 μm.
95% of Particles Fall between 2.94 and 19.89 μm.
Slope of Probability Curve: 0.4873 T Test: 25.51
Slope of Bottom Half: 0.6132 Median: 8.47 T = 46,170.40
Slope of Top Half: 0.3954 Median: 8.97 T = 580.63

EMULSIFICATION TIME

If the Sauter mean diameter is plotted against the reciprocal of the time, a nearly straight line is achieved after about 120 minutes of agitation. Extrapolating this line to infinite time (the intercept) gives that ultimate diameter. This was demonstrated by Fondy and Bates (1963). The data for Batch 9 are plotted this way in Figure 2. If the ultimate diameter subtracted from the mean diameter is

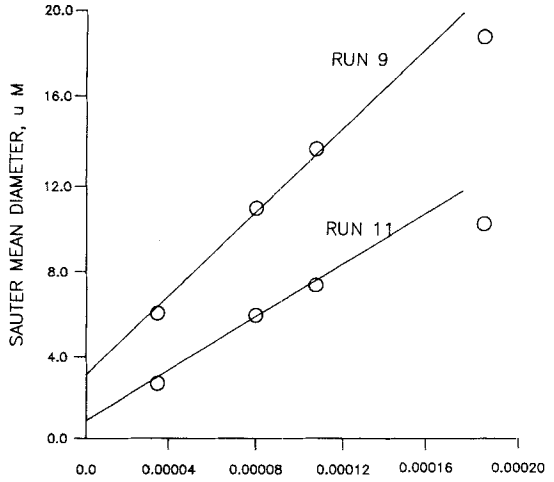

Figure 2. Extrapolation of emulsion size as a reciprocal of time.

plotted on semilog paper against time, the result is a very good fit even at the earliest times, Figure 3. This shows that the ultimate diameter is exponentially approached and the slope of this curve is the reiprocal of the time constant. This has been calculated for all of the data, Table 1. The value of the intercept was calculated for each time beyond 90 minutes from the graphically determined slope. These intercepts were then averaged to give the value in the table. Ideally an iterative procedure on the ultimate diameter would give a better fit of the data but this is not practical within the range of measurement errors encountered. Thus only one iteration is used. Table 1 shows that time constants of 50 to about 150 minutes are observed in our system. This means that 63.2% of the remaining change is observed during the period of one time constant.

It is instructive to correlate the ultimate diameter to the independent variables that were measured. This results in the following correlation with a F-test of 64:

$$d_u = \frac{1.214 \times 10^{15}}{U^{6.84}T^{1.73}}$$

This correlation gives a stronger response of turbine tip speed (U) on the ultimate diameter than observed by Fondy and Bates for a *fixed time* observation.

It was also found that the ultimate diameter was related inversely to the emulsification temperature to the 1.7 power. The temperature was included as a way to compensate for small temperature changes and not to define property changes resulting from the temperature level. Because of the relation of power and speed, the change in temperature will affect the power because of viscosity and surface tension changes at the same tip speed. Therefore, different exponents can be expected on the temperature when correlated with tip speed as opposed to a correlation with power consumed.

The rate with which the distribution approaches the ultimate diameter has been determined from the slope of the curve for the mean diameter vs. the reciprocal of time as well as the time constant. This slope is given in the next to the last column of Table 1 and can be considered as an inverse function of the time constant. Correlations of both were attempted with the slope giving the best correlation. The slopes were correlated at the 95% level ($F = 7.4$) by the equation:

$$\text{Slope} = \frac{3.517T^{0.568}U^{0.557}}{p^{0.761}}$$

Since Power is proportional to the cube of the tip speed:

$$\text{Slope} = f\left(\frac{U^{0.557}}{(U)^{3(0.761)}}\right) = f(U^{-1.726})$$

This shows that a faster change (higher slope) is obtained with higher temperatures and liquid volumes but slower change results from high power levels. For the rate of approach to the ultimate

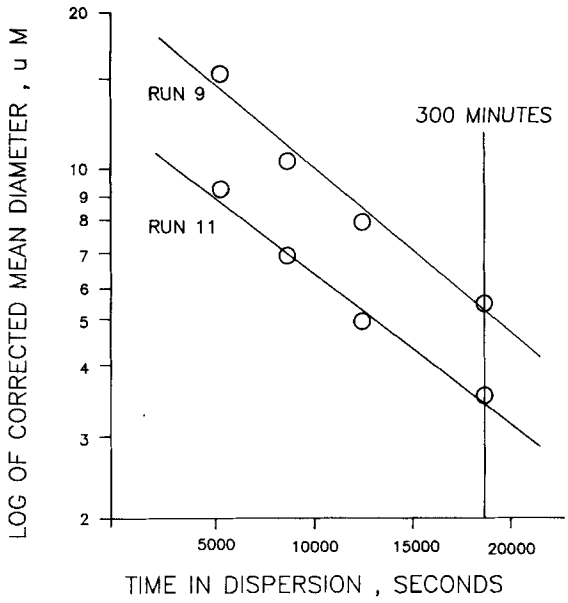

Figure 3. Change in the log of corrected diameter with time.

diameter, Fondy and Bates observed that the mean diameter varied with tip speed to the −1.8 power. Our overall correlation of mean diameter at a fixed time shows an exponent of (−1.73) as can be noted in the equation for the slope given above.

It has been noted that the ultimate diameter is primarily controlled by the tip speed (and temperature). Changes in other parameters such as turbine shape, volume in tank, and fluid properties have only a minor effect. They do, however, determine how quickly this ultimate diameter is reached. Therefore, the effects of these other parameters should be understood.

VOLUME EFFECTS

The diameters obtained after 300 minutes of dispersion have been plotted for the 150-mm-diameter impeller in Figure 4. It shows that the Sauter diameter reaches a minimum for all speeds at about 19 L in the tank. The same shaped curves are produced by the ultimate diameter as a function of volume except for the highest speed at the lowest volume, where the diameter differences

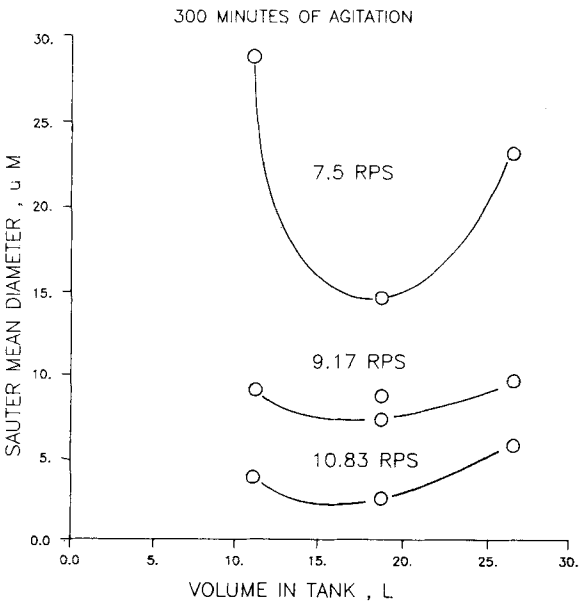

Figure 4. Effect of tank level on emulsion size.

are as large as the scatter. This minimum corresponds to a level of about 295 mm of emulsion in the tank. Since the tank is 285 mm in diameter, this corresponds to roughly a height equal to the diameter. The data show that high liquid volumes produce lower energy input per unit volume. It appears that above the optimum liquid volume, power remains constant while with more liquid the power is spread over a greater volume. At lower liquid levels, total energy consumption decreases as gross turbulence and surface activity appear. Although the power per unit volume seems to remain the same (at constant tip speed), much of the energy is wasted on turbulence. The emulsification comes primarily from the vortices shed from the turbine tip, not in gross turbulence.

OTHER VARIABLES

A floating cover was added to the tank to prevent surface activity and air entrainment into the vortex systems. Runs 25 and 38 were made under these conditions. A comparison between these and Runs 16 and 35 show that the total power dissipation was not significantly changed but that the mean drop size was markedly decreased.

In Runs 23 and 24, a marine type impeller was used in place of same size flat turbine (Run 22). The vortex shedding from the marine impeller is completely different from that of a turbine. Because of the large pumping action of the marine impeller, the vortices probably receive less power input than those of the flat blade turbine. They tend to be a continuous trailing flow pattern below the propeller, and, as a result, are more coherent and less effective in emulsion production. Examination and comparison with the equivalent Run 22 for the turbine show no practical change in mean drop diameter and a very small reduction in power consumption. Because of the large amount of gross turbulence produced by the marine impeller, it is not an attractive substitute for the flat-bladed turbine.

The number of vortices formed by an impeller is in proportion to the number of blades on the impeller. Our basic turbine contained six blades which is typical of a flat turbine. A second turbine having 12 blades was fabricated and used in the last nine runs (41–49). As expected, the 12-blade impeller allowed us to put more power into the emulsion at the same tip speed. This resulted in substantially smaller mean particle diameters. For the 12-bladed impeller, the blade shape was changed slightly by machining 8 mm from the top or bottom of alternate blades. This produced as many vortices, but would not have the same amount of pumping action and gross turbulence. Comparing Runs 46–49 with Runs 22 and 28 show that the power consumption is reduced at the same speed but that the mean drop diameter remains about the same. Thus, turbine design can be an important factor in effective emulsification. The increasing number of blades has a practical limit when the vortex from one blade tip interferes with the vortex from another tip. For this reason, the staggered blades are an attractive way to solve this problem.

NOTATION

A = particle surface area, m^2
d_I = impeller diameter, m
d_u = ultimate diameter (Sauter mean), μm
d_{32} = Sauter Mean diameter, μm
N = impeller speed, rps
P = power dissipated by impeller, N·m/s = W
t = time, s
T = temperature, °C.
U = tip speed, m/s
V = volume in vessel, L
σ = interactial tension, N/m
μ = viscosity, N·s/m^2

LITERATURE CITED

Brodkey, R., "The Phenomena of Fluid Motions," Ch. 17.3, Addison Wesley, MA (1967).

Chang, T. P. K., Y. H. E. Sheu, G. B. Tatterson, and D. S. Dickey, "Liquid Dispersion Mechanism in Agitated Tanks: and Part II. Straight Blade and Disc Style Turbines," *Chem. Eng. Commun.*, **10**, p. 215 (1981).

Fondy, P. L., and R. T. Bates, "Agitation of Liquid Systems Receiving a High Shear Characteristic," *AIChE J.*, **9**, p. 338 (1963).

Keey, R. B., and J. B. Glen, "Area-Free Mass Transfer Coefficients for Liquid Extraction in a Continuously Worked Mixer," *AIChE J.*, **15**, p. 942 (1969).

Lapple, C. E., "Particle-Size Analysis and Analyzers," *Chem. Eng.*, **70**, No. 10, p. 149 (1963).

Mlynek, Y., and W. Resnick, "Drop Sizes in an Agitated Liquid-Liquid System," *AIChE J.*, **18**, p. 122 (1972).

Rushton, J. H., "Interfacial Synthesis,' F. Millick and C. E. Carraher, Jr., eds., p. 44, Marcel Dekker, Inc., New York (1977).

Shinnar, R., "On Behavior of Liquid Dispersions in Mixing Vessels," *J. Fluid Mech.*, **10**, p. 259 (1961).

Sprow, F. B., "Distribution of Drop Sizes Produced in Turbulent Liquid-Liquid Dispersion," *Chem. Eng. Sci.*, **22**, p. 435 (1967).

Thronton, J. D., and B. A. Bouyatiotis, "Liquid-Extraction Operations in Stirred Vessels," *Ind. Chemist*, **39**, p. 298 (1963).

Van't Riet, K., and J. M. Smith, "The Training Vortex System Produced by Rushton Turbine Agitators," *J. Eng. Sci.*, **30**, p. 1093 (1975).

ACKNOWLEDGMENT

The major part of the laboratory work for this study was carried out by Joel Timberlake, a co-op student from Georgia Tech and was completed by Jack Steffy, a senior technician at Mead.

Manuscript received January 22, 1982; revision received May 3, and accepted August 27, 1982.